Temperature-dependent optical properties of InAs/GaAs quantum dots: Independent carrier versus exciton relaxation

P. Dawson,[1,*] O. Rubel,[2] S. D. Baranovskii,[2] K. Pierz,[3] P. Thomas,[2] and E. O. Göbel[3]
[1]*School of Physics and Astronomy, University of Manchester, Sackville Building, Manchester, England*
[2]*Department of Physics and Material Sciences Center, Philipps-University Marburg, Renthof Str. 5, D-35032 Marburg, Germany*
[3]*Physikalisch-Technische Bundesanstalt, Bundesallee 100, D-38116 Braunschweig, Germany*
(Received 1 July 2005; revised manuscript received 16 September 2005; published 2 December 2005)

We have performed temperature-dependent studies of the photoluminescence properties of a range of InAs/GaAs quantum dot structures. Changes in the temperature dependence of the peak energy and spectral width are governed by thermally stimulated transfer processes and hence depend on the depth of the confining potentials. We have compared our experimental results with detailed calculations based upon correlated electron-hole (exciton) or independent electron-hole relaxation. We conclude that at elevated temperatures the carrier dynamics are governed by independent carrier relaxation.

DOI: 10.1103/PhysRevB.72.235301 PACS number(s): 78.67.Hc

I. INTRODUCTION

It has been demonstrated that nanometer-sized semiconductor quantum dots can be fabricated in a wide range of material systems by making use of the Stranski-Krastanov coherent island growth mode (self-organized growth). Quantum dots fabricated using the InAs/GaAs system have been widely studied and can be regarded as a model system. In particular, the optical properties have been studied in detail; comprehensive reviews can be found in the work by Bimberg *et al.*[1] and Skolnick *et al.*[2] As the field has developed the techniques used to investigate, such systems have become increasingly complex and detailed, culminating in the study of single quantum dots. On the other hand, the study of the optical properties of an ensemble of quantum dots can reflect the general behavior of a disordered electronic system and, in addition, is of direct relevance for the application of such systems, e.g., in quantum dot lasers. Such studies are also of value for other related systems, for example, in quantum wells where the carriers are highly localized, such as in the $In_xGa_{1-x}N/GaN$ system.[3]

The study of the temperature dependence of the optical properties of a quantum dot ensemble can be particularly revealing giving information on how optically injected carriers are distributed within the ensemble and the processes which govern the distribution. In general, in photoluminescence experiments where the excitation density is sufficiently low that only recombination occurs from the InAs/GaAs quantum dot ground states, the low temperature spectrum consists of an inhomogeneously broadened line with peak energy $\simeq 1$ eV.[4] The most widely studied temperature-dependent parameters of the photoluminescence spectra are the peak energy, E_p, the full width at half maximum (FWHM) height, and the integrated intensity. It has been found[5–14] that at low temperatures ($T < 100$ K) the peak energy can decrease more rapidly as a function of temperature than might be expected if the change was governed solely by the change in the band gap of InAs. Furthermore it has been observed that the FWHM of the spectrum can also decrease as the temperature is raised up to some critical temperature followed by an increase at higher temperatures. The photoluminescence intensity remains essentially constant in the low temperature regime but decreases as the temperature is increased further. It should be stressed that the precise behavior observed depends on such parameters as the low temperature peak energy and the composition, and hence band gap, of the barrier material. Qualitatively this behavior can be explained as follows. As the temperature is increased the carriers that are in less, well-confined quantum dots, i.e., those in the smaller quantum dots that contribute to the high energy part of the photoluminescence spectrum, are thermally emitted to the barrier and/or wetting layer and subsequently retrapped or lost through nonradiative or radiative recombination in the barrier layers. Thus as the temperature is increased the linewidth is reduced and the peak energy gradually shifts to lower energies until the temperature is sufficiently high that the carriers are thermally distributed across all the quantum dot states. Although this general behavior is widely reported it is, nevertheless, not universal. As noted by Heitz *et al.*,[15] and confirmed by our results, the photoluminescence spectra do not always show the pronounced reduction in FWHM and the associated shift to low energy of the peak energy with increasing temperature. Instead, the behavior is different for samples with different E_p and hence different average confinement energies with the general trend that temperature effects on E_p and the FWHM of the spectra are less pronounced for samples with lower E_p, i.e., larger confinement.

The theoretical modeling of the optical properties of an ensemble of quantum dots is usually based on a set of rate equations which describe the dynamics of the carrier exchange between the quantum dots and the barrier via the wetting layer.[10,11] It is usually assumed that the carriers behave as correlated electron-hole pairs (excitons) during the thermally stimulated redistribution processes. However, so far, there is no direct experimental evidence for such an assumption. Such excitonic models, which are widely used in the interpretation of experimental data, are attractive possibly because of their relative simplicity.[16,17] In this paper we compare the results of a theoretical model with the measured

temperature-dependent optical properties of a range of InAs/GaAs quantum dot structures with E_p varying between 1.04 and 1.23 eV. The model includes the following physical effects that have not always been included in models used previously.

(1) In contrast to most previous models, we consider specifically the effects of exciton or independent carrier relaxation.

(2) We consider the redistribution of charge carriers between the quantum dot bound states to occur via the GaAs barrier continuum states. In previous models[10,11] such a process was neglected in favor of carrier exchange via the wetting layer; we believe this results in the carrier escape rate from the quantum dots being underestimated.

(3) The energy differences between the quantum dot states and the matrix (defined as the confinement energies) are not used as fitting parameters but are calculated as a function of dot size following the treatment of Barker and O'Reilly.[18]

(4) When calculating the photoluminescence spectrum we take into account the natural anticorrelation of the confinement energies of the electron and hole states caused by the variation of the dot size. This means that smaller quantum dots have smaller confinement energies for both electron and hole states. This, in particular, is in contrast to the work of Lee *et al.*[10] and Sanguinetti *et al.*[11] where the relative energy distribution of two recombining carriers was allowed to be random.

The paper is organized as follows. In Sec. II we present details of the sample growth and the optical measurements. The results from the studies of the temperature-dependent optical properties are presented in Sec. III. In Sec. IV we derive a set of rate equations that describe the carrier dynamics in the quantum dots. The experimental results are discussed in detail for the two alternative theoretical models in Sec. V. The main results of our work are summarized in Sec. VI.

II. EXPERIMENTAL DETAILS

The samples were grown by molecular beam epitaxy on semi-insulating GaAs(100) wafers. Both samples whose optical properties are reported in detail consist of the same layer sequence, however, the quantum dots in sample No. 617 were grown at 480 °C while those in sample No. 592 were grown at 530 °C. The growth sequence of the constituent layers was as follows. First a 500 nm thick buffer layer of GaAs was grown at a temperature of 600 °C, followed by a ten period superlattice of 2.5 nm GaAs and 2.5 nm AlAs. Then a single layer of InAs quantum dots confined by 30 nm thick GaAs barriers was grown. After growth of the first GaAs barrier the wafer rotation was stopped and during a 2 min growth interruption the temperature was reduced to the required temperature (T_s=480 °C or 530 °C) for the quantum dot growth. The growth of the quantum dots was achieved by depositing 2 ML of InAs at a rate of 0.05 ML/s. The formation of the quantum dots was observed by monitoring the reflection high-energy electron diffraction image which changed from a streaky to a spotty pattern after deposition of ≈1.5 ML of InAs. After the growth of the quantum dots and a 30 s pause in growth the second GaAs barrier was grown while gradually increasing the temperature up to T_s =600 °C. Finally another ten period superlattice of 2.5 nm GaAs and 2.5 nm AlAs was grown followed by a 10 nm thick cap layer of GaAs. The superlattice structures were incorporated to reduce the loss of the photogenerated carriers to either the free surface or to the substrate. For the photoluminescence measurements the samples were mounted on the cold finger of a variable temperature closed cycle cryostat and excited by the chopped light from a He/Ne laser. The emission was analyzed and detected by a 1 m grating spectrometer followed by a cooled North Coast Ge detector and lock-in amplifier. The maximum and minimum excitation power densities used were 0.01 W cm^{-2} and 160 W cm^{-2}. Assuming that all the photoexcited electron-hole pairs are captured by the quantum dots and that the recombination time is 1 ns, we estimate that the maximum carrier density in the quantum dots ranged between 2×10^{7} cm^{-2} and 5×10^{11} cm^{-2}. As shown in Fig. 1 even at the highest excitation density the spectra consisted of a single line with no evidence of any features at high energy, thus in our analysis we ignored any occupation of the excited states of the quantum dots due to state filling effects. Furthermore, to ensure meaningful comparison with the calculations, the maximum temperature up to which measurements were taken was dictated by the absence of any high energy feature in the spectra caused by recombination involving the thermal occupation of the excited states.

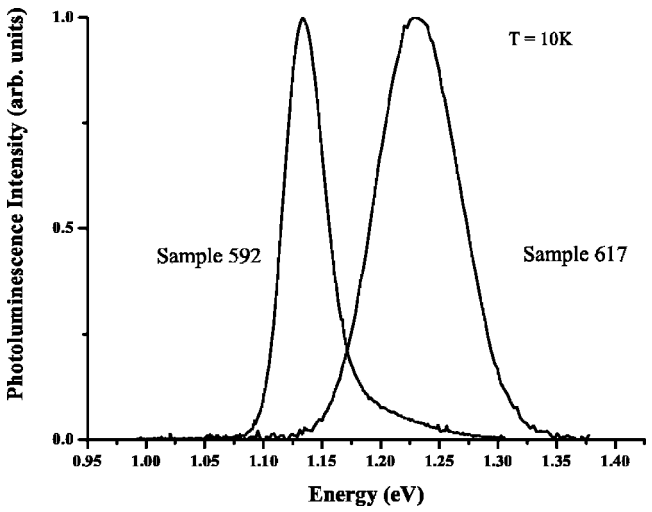

FIG. 1. Photoluminescence spectra of sample Nos. 592 and 617 recorded at a temperature of T=10 K for the highest excitation power density.

III. EXPERIMENTAL RESULTS

We studied in detail six samples with E_p at 10 K varying between 1.038 and 1.227 eV. Thus, as will be discussed in detail later, the average confinement energies of the electrons and holes are different from sample to sample. The temperature dependence of the spectra and the integrated photoluminescence intensity were studied in detail; for the sake of

clarity not all the results obtained are shown or discussed in detail, we only note the following general observations. The change in peak energy as a function of temperature showed a systematic behavior as a function E_p. For the samples with E_p in the range 1.038 to 1.135 eV the peak shift was in good or reasonable agreement with what might be expected from the temperature variation of the InAs band gap. Whereas for samples with $E_p \geqslant 1.181$ eV, i.e., those with the lowest average carrier confinement, the peak energy decreased more rapidly than the temperature dependence of the InAs band gap, in fact, the greater the value of E_p the greater the shift in the peak energy. For the samples with a peak energy $\leqslant 1.135$ eV the FWHM either remained relatively constant or showed a smooth decrease with increasing temperature; whereas, the samples with peak energies $\geqslant 1.185$ eV exhibited a decrease in FWHM with increasing temperature until a temperature around 120 K above which the FWHM then increased.

In general, increases in E_p are ascribed to reductions in the carrier confinement energies due to decreases in the average size of the quantum dots. Thus, as E_p increases, the effects of thermally stimulated carrier escape become increasingly important. Depending on the value of E_p the samples can be split into two groups, i.e., those with $E_p \leqslant 1.135$ eV and those with $E_p \geqslant 1.135$ eV. So for the temperature range we have studied, the effects of carrier escape are most significant for those samples with E_p less than 1.135 eV. To illustrate this behavior the results for sample Nos. 592 (E_p=1.105 eV) and 617 (E_p=1.23 eV) are presented in detail in Fig. 2.

Shown in Fig. 2(a) is the variation of E_p for these two samples with the lowest and highest excitation power density. It should be noted that the data have been corrected to reflect only changes in E_p due to relaxation and thermalization so the expected change in the band gap of InAs has been removed using Varshni's equation incorporating the constants provided by Vurgaftman *et al.*[19] As can be seen the change in E_p for sample No. 592 for both excitation power densities are very similar and are much less pronounced than both sets of data for No. 617. Also the change in E_p for No. 617 taken with the lower excitation power density is more pronounced than that at the high excitation power density. Shown in Fig. 2(b) is the temperature dependence of the FWHM of the spectra at both low and high excitation power densities. The FWHM as a function of temperature for No. 592 remains relatively unchanged with increasing temperature for both excitation power densities. The FWHM for No. 617 decreases then increases with the minimum in the FWHM occurring around 140 K whereas the high power data show similar behavior except that the minimum occurs around 170 K. Last, in Fig. 2(c) the normalized integrated photoluminescence intensities for Nos. 592 and 617 are shown as a function of temperature for both low and high excitation densities. The normalized integrated intensity of No. 592 is essentially independent of excitation power density and decreases by about a factor of 2 on increasing the temperature from 10 to 200 K. Whereas the normalized integrated intensity of No. 617 remains relatively constant up to temperature around 70 K, but then falls much more rapidly; with the low excitation power density data falling off most rapidly.

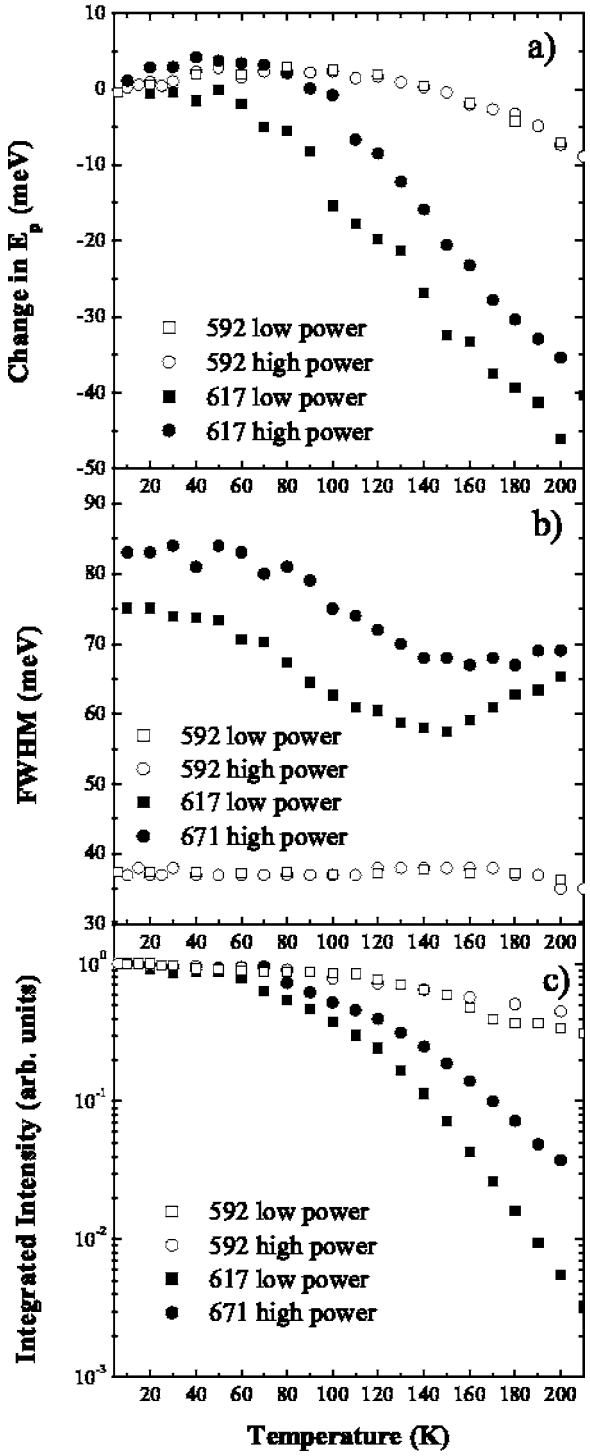

FIG. 2. Experimental data for the relative photoluminescence peak energy (a), the FWHM of the spectra (b), and the integrated photoluminescence intensity (c) for sample Nos. 617 and 592 at the indicated excitation densities.

IV. THEORETICAL MODEL

A. Rate equations

To interpret the experimental results, we use a set of rate equations similar to those suggested in Refs. 10 and 11, although, as was outlined earlier, with some significant modi-

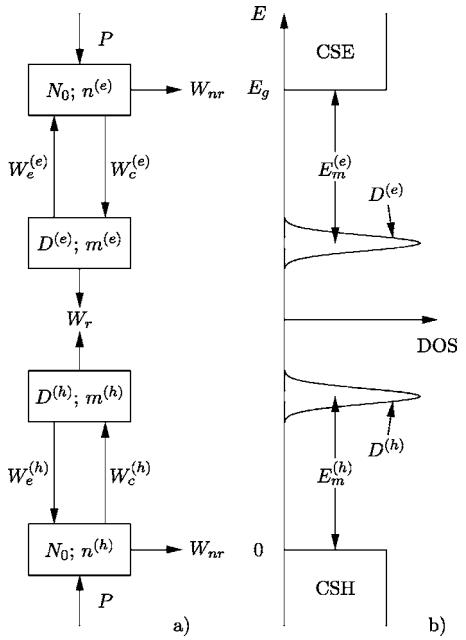

FIG. 3. Schematic rate equation model (a) and the band DOS diagram (b) for quantum dots. Where P denotes the pumping rate; W_{nr} is the nonradiative recombination rate for charge carriers in the barrier; W_c is the carrier capture rate into quantum dots; W_e is the carrier thermal escape rate; N_0 is the concentration of continuum states in the barrier; n is the carrier concentration in the barrier; D is the density of quantum dot states; m is the carrier concentration in quantum dots; E_g is the band gap in the barrier material. The average confinement energies for electron and hole ground states are denoted by $E_m^{(e)}$ and $E_m^{(h)}$, respectively. CSE and CSH denote continuum states for electrons and holes in the barrier, respectively.

fications. In line with previous works, we will consider InAs quantum dots with a two-dimensional density N_D located in a GaAs matrix. We do not include any direct carrier transfer mechanisms between the quantum dots such as tunneling, and only permit exchange of electrons and holes to occur via thermal activation to states in the barriers. Also, as mentioned above, we consider the escaping carriers as either excitons or independent electrons and holes. In the latter case, the occupation of quantum dots by electrons and holes is only correlated via the recombination terms in our equations, which explicitly depend on the independent electron and hole occupation factors. In work previously published the recombination term using an exciton model was assumed to be dependent on the occupation factor of only one kind of carrier, i.e., either electrons or holes. This implies that the recombination partner for an electron or a hole is always present in a quantum dot. This assumption, in particular, at low excitation density, is, however, not appropriate for the treatment of the processes necessary to account accurately for the temperature-dependent effects.

The general scheme of our model for the case of independent carrier relaxation is shown in Fig. 3. In the model we consider only the ground states of the quantum dots, since in our experiments no photoluminescence was observed from the excited states. The ground-state energies have some distribution caused primarily by variations in the size of the quantum dots.[18,20] The distribution function for the ground-state energy levels of electrons and holes in the quantum dots is assumed to be Gaussian

$$D(z) = \frac{1}{\sqrt{2\pi}} \exp\left(-\frac{z^2}{2}\right). \tag{1}$$

We use renormalized energies z related to the hole energies $E^{(\mathrm{h})}$ via $E^{(\mathrm{h})}=E_m^{(\mathrm{h})}-zE_0^{(\mathrm{h})}$ and to the ground-state energies of the electrons, $E^{(\mathrm{e})}$, in the quantum dots via $E^{(\mathrm{e})}=E_g-E_m^{(\mathrm{e})}+zE_0^{(\mathrm{e})}$. Where E_g is the band gap of the barrier material, E_m is the energy difference between the maximum of the distribution of the ground-state energies and the band edge of the barrier and E_0 is the standard deviation. The superscripts (e) and (h) are used to identify the functions for electrons and holes.

Let us consider a system of quantum dots in a semiconductor matrix where electron-hole pairs are generated continuously mainly in the matrix at a pump rate P [see Fig. 3(a)]. Let n be the steady state concentration of electrons (holes) in the matrix. These carriers can undergo two possible processes: recombine at a rate of

$$W_{nr}^{(\mathrm{e,h})} = R' n^{(\mathrm{e,h})}, \tag{2}$$

or be captured by the quantum dots at a rate of

$$W_c^{(\mathrm{e,h})}(z) = R_c n^{(\mathrm{e,h})} D(z)[1 - f^{(\mathrm{e,h})}(z)], \tag{3}$$

where R' and R_c are the sum of the nonradiative and radiative recombination rates in the barriers and the capture rate coefficients, respectively, and $f(z)$ is the occupation probability of the quantum dot states.

Carriers captured into the quantum dots can then undergo two further processes: they can either be thermally activated into the barrier layer at a rate

$$W_e^{(\mathrm{e,h})}(z) = R_c N_0 D(z) f^{(\mathrm{e,h})}(z) \exp\left[\frac{-E_a^{(\mathrm{e,h})}(z)}{kT}\right], \tag{4}$$

or recombine radiatively at a rate

$$W_r(z) = R N_D D(z) f^{(\mathrm{e})}(z) f^{(\mathrm{h})}(z), \tag{5}$$

where N_0 denotes the density of GaAs barrier states, N_D is the areal density of quantum dots (QDs), E_a is the activation energy for thermal escape, and R is the rate coefficient for radiative recombination in the quantum dots.

In order for the radiative recombination to occur in a quantum dot, both the electron and hole ground states in a particular quantum dot should be occupied. Therefore, Eq. (5) contains the product of the occupation probabilities for the electron and hole states in the quantum dots. It is the form of this equation that makes our model different from the majority of the previous theoretical treatments where the recombination was assumed to be dependent on only one occupation probability function. This assumption overestimates the recombination rate at elevated temperatures by orders of magnitude, since one occupation function in Eq. (5) is always taken as unity.[10,11]

The value of the activation energy, E_a, in Eq. (4) is equal to the difference between the ground-state energy in a quantum dot and the band edge energy of the barrier. It can be

expressed in the form $E_a^{(e,h)}=E_m^{(e,h)}-zE_0^{(e,h)}$. In general, electrons and holes have different activation energies reflecting the asymmetry of the band offsets which automatically leads to different confinement energies E_m. Therefore as the escape rates are determined mainly by the confinement energies they will be different for electrons and holes and the assumption of equal escape rates used in most previous models is not justified.

Furthermore, the anticorrelation between the ground-state energies for electrons and holes in a quantum dot is taken into account in Eq. (5). This anticorrelation arises due to the effect of the quantum dot size on the confinement energies. The smaller the quantum dot, the larger the energy difference between the electron and hole ground states in the dot. This effect is also taken into account in our calculations.

The time evolution of the carrier concentrations in the barrier, n, and in the quantum dots m are described by the set of rate equations:

$$\frac{dn^{(e)}}{dt} = P - W_{nr}^{(e)} - \int dz\, W_c^{(e)}(z) + \int dz\, W_e^{(e)}(z), \quad (6a)$$

$$\frac{dm^{(e)}(z)}{dt} = W_c^{(e)}(z) - W_e^{(e)}(z) - W_r(z), \quad (6b)$$

$$\frac{dn^{(h)}}{dt} = P - W_{nr}^{(h)} - \int dz\, W_c^{(h)}(z) + \int dz\, W_e^{(h)}(z), \quad (6c)$$

$$\frac{dm^{(h)}(z)}{dt} = W_c^{(h)}(z) - W_e^{(h)}(z) - W_r(z). \quad (6d)$$

This is a system of two sets of nonlinear equations for electrons and holes and describes the system that is shown schematically in Fig. 3(a). The set of equations is general and is valid for all regimes of carrier generation. The rate equations for the electrons and holes cannot be solved independently since they are coupled via the radiative recombination terms W_r, which contain information on the occupation of the quantum dots by electrons and holes. Our experiments, however, were carried out under continuous excitation conditions and therefore we restrict our theoretical analysis by considering only a steady state system which implies $dn/dt=0$ and $dm/dt=0$. The solution of Eqs. (6) is the combination of the population functions $f(z)$ for electrons and holes in the quantum dots for the given generation rate P. The calculated population functions are then used to derive the photoluminescence spectra via the following expression:

$$I(z) \propto D(z) f^{(e)}(z) f^{(h)}(z), \quad (7)$$

which is consistent with Eq. (5). It should be noted that an expression similar to Eq. (7) can be also found in Ref. 10. However the recombination term in Ref. 10 differs from Eq. (5) being dependent on the population function of only one type of carrier, i.e., electrons or holes. This means that the equations for holes and electrons in Ref. 10 are decoupled from each other and hence their model is significantly different from that presented here.

The photoluminescence intensity $I(z)$ described by Eq. (7) is associated with the photoluminescence energy $E_{PL}(z)$ via the renormalized energy z as

$$E_{PL} = E_g - E_m^{(e)} - E_m^{(h)} + z[E_0^{(e)} + E_0^{(h)}]. \quad (8)$$

The last term in Eq. (8) includes the anticorrelation effect for the energies of recombining electrons and holes.

We use the model to predict the variation of the three characteristic features of the photoluminescence spectrum: E_p, its FWHM, and the integrated intensity as a function of temperature. The photoluminescence peak energy E_p is determined as the first moment of the photoluminescence spectra

$$E_p = \frac{\int dE\, EI(E)}{\int dE\, I(E)}. \quad (9)$$

The FWHM ΔE of a photoluminescence spectrum is calculated assuming that it has a form close to that of a Gaussian function. Therefore ΔE is given by

$$\Delta E = 2\sqrt{2 \ln 2}\left[\frac{\int dE(E-E_p)^2 I(E)}{\int dE\, I(E)}\right]^{1/2}. \quad (10)$$

The integrated photoluminescence intensity is calculated by the integration of $I(z)$ over the whole energy range.

B. Exciton model

One of the most important issues is whether the electrons and holes transfer between the quantum dots and the matrix as excitons or do they act as independent electrons and holes and only recombine when they occupy a quantum dot that is already occupied by a carrier of the opposite sign. To clarify this problem in Sec. V we compare the theoretical conclusions of our model for uncorrelated electrons and holes from Sec. IV A with those of the excitonic model described by Sanguinetti *et al.*[11] In the exciton model it is assumed that the electrons and holes are strongly correlated and thus they always relax or are thermally released together. This assumption dictates that the term responsible for the radiative recombination in Eqs. (6b) or (6d) has to be replaced by the exciton recombination rate

$$W_r(z) = RN_D D(z) f(z), \quad (11)$$

where $f(z)$ refers to the distribution function of a carrier (electron or hole) with the larger activation energy. As a consequence of Eq. (11) the photoluminescence intensity in the exciton model can be expressed in the form

$$I_{exc}(z) \propto D(z) f(z). \quad (12)$$

Hence it is necessary to solve Eq. (6) for only one type of carrier, namely that with the larger activation energy.

TABLE I. Parameters used to calculate the photoluminescence spectra.

Parameter	Value	Dimension
N_D	10^{10}	cm^{-2}
N_0	10^{14}	cm^{-2}
R_c	3×10^{10}	s^{-1}
R	10^{9}	s^{-1}
R'	10^{9}	s^{-1}

V. RESULTS AND DISCUSSION

To perform calculations using the set of rate equations described above we need to specify the values of the parameters to be used. For the rate coefficients R, R', and R_c the values we use are given in Table I and are taken from Refs. 10 and 11; these values also agree with those found experimentally.[21,22] The value we use for the density of extended states in the barrier regions is $N_0 \approx 10^{14}$ cm^{-2}, which corresponds to the conventional three-dimensional concentration of 10^{21} cm^{-3}. For simplicity we assume equal densities of states for the valence and conduction bands, although in reality they are slightly different due to the difference in effective masses. In Ref. 10 it was assumed that the carriers escape into the two-dimensional wetting layer which has an associated low density of states. Therefore, a very low value of the activation energy for the escape from the quantum dots was necessary for agreement with the experimental data.[10] In Ref. 11 the two-dimensional concentration of states in the barrier was assumed to be larger than 10^{17} cm^{-2}. Such a value of N_0 seems too high for a two-dimensional system.

The ground-state confinement energies E_m for the electrons and holes depend mainly on the size of the quantum dots,[18] d. In the limit $T\rightarrow0$ K, assuming random capture probability, the value of E_p is the recombination energy for those quantum dots with the greatest density of states. Therefore, the photoluminescence peak energy is related to the confinement energies, E_m, and the barrier band gap E_g by $E_p=E_g-E_m^{(e)}(d)-E_m^{(h)}(d)$. For sample No. 617 $E_p=1.227$ eV at $T=6$ K and using a value for the band gap of GaAs at $T=6$ K of 1.52 eV gives a value for the sum of the electron and hole confinement energies of 0.303 eV. Then using the results of Ref. 18 for the confinement energies for ideal pyramidal quantum dots, one can determine the individual confinement energies for electrons and holes and the quantum dot size, d, yielding $E_m^{(e)}=0.15$ eV and $E_m^{(h)}=0.15$ eV and $d\approx9.5$ nm. For sample No. 529 a similar analysis yields the quantum dot size $d\approx13$ nm that corresponds to confinement energies $E_m^{(e)}=0.23$ eV and $E_m^{(h)}=0.19$ eV.

We assume that the distribution of ground-state energies is caused primarily by size fluctuations. To derive E_0 for sample No. 617 we examined the slopes of the curves E_m vs d in the range $9<d<10$ nm (see Fig. 1 of Ref. 18), thus we obtained values for the slopes for electrons and holes of 0.026 eV/nm and 0.012 eV/nm, respectively. Therefore, we conclude that for this particular sample the electron confinement energy is much more sensitive to the variation of quantum dot size than hole confinement energy, $E_0^{(e)}\approx2E_0^{(h)}$. Fitting the FWHM of the photoluminescence spectrum at $T=6$ K we obtain $E_0^{(e)}=21$ meV and $E_0^{(h)}=10.5$ meV, which corresponds to a standard deviation of the quantum dot size of the order of 1 nm.

The results of our calculations using the exciton and the independent electron and hole models are shown in Figs. 4–7 for the two samples that we have studied experimentally in detail. For the high and low excitation density measurements the quantum dot carrier density generation rates were $P=10^{19}$ cm^{-2} s^{-1} and $P=10^{16}$ cm^{-2} s^{-1}, respectively. In the graphs of the peak energy of the spectra versus temperature we have considered only changes caused by the effects of carrier redistribution and not any changes caused by the temperature dependence of the band gaps of GaAs and/or InAs. This is consistent with the plots of the experimental data in Fig. 2(a). For both models the calculated photoluminescence spectra reproduce qualitatively the main features that are commonly observed in the optical properties of quantum dots with increasing temperature, i.e., a quenching of the photoluminescence intensity and a redshift and narrowing of the photoluminescence spectrum over a specific temperature range. However, there are significant differences in the detail of the predictions of exciton and independent electron and hole models, in particular, concerning the thermal quenching of the photoluminescence intensity at different excitation intensities. We start our detailed discussion by comparing the observed and predicted properties of sample No. 617 (Figs. 2, 4, and 5) with the predictions of the model for independent electrons and holes. At low excitation density the independent electron and hole model predicts the following (Fig. 4). The photoluminescence spectra are temperature independent for temperatures below $\approx$80 K.

At such low temperatures the thermal escape of charge carriers from the quantum dots into the barriers does not occur at a sufficiently fast rate compared to the radiative lifetime of carriers in the quantum dots. Hence the electrons and holes that are randomly captured by the quantum dots remain there until a carrier of the opposite charge appears in the same dot and recombination occurs. Therefore, radiative recombination from the quantum dots is the dominant recombination mechanism in this temperature range. With increasing temperature some carriers are thermally activated into the barrier states giving rise to either nonradiative or radiative recombination in the barriers. This results in the reduction of the predicted photoluminescence intensity for temperatures greater than 100 K. The carriers, which are less susceptible to these thermally activated recombination paths in the barriers, are those that are located in the quantum dots with the largest confinement energies. This explains the rapid shift of the photoluminescence peak towards lower energy and the reduction of the photoluminescence linewidth in the temperature range between 80 and 140 K [Figs. 4(a) and 4(b)]. The reduction of the relative shift of the photoluminescence peak for temperatures above $\sim$170 K at the lower excitation rate can be attributed to the effect of a Boltzmann distribution of charge carriers in the quantum dots. The combination of the Gaussian density of states (DOS) and the Boltzmann distribution gives a population function with a peak shifted with respect to the DOS peak by an energy of

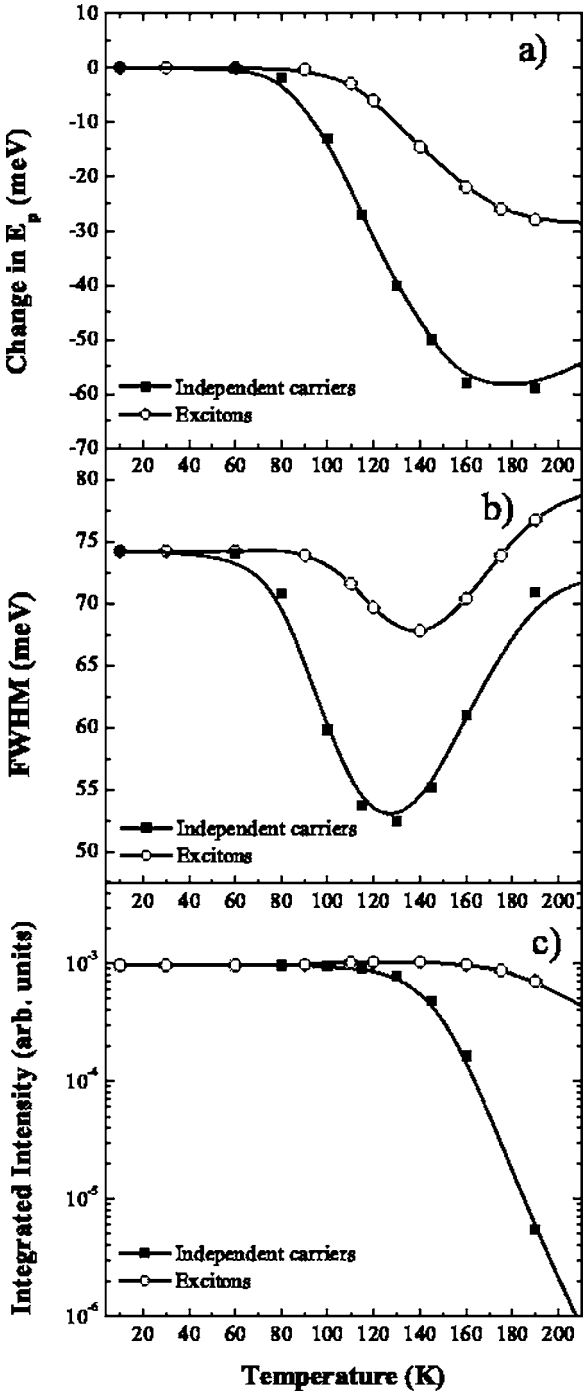

FIG. 4. Relative photoluminescence peak energy (a), the FWHM of the spectra (b), and integrated photoluminescence intensity (c) as a function of temperature calculated for sample No. 617 at the low excitation rate of $P=10^{16}$ cm^{-2} s^{-1}. Open circles and filled boxes correspond to the excitonic and nonexcitonic models, respectively. In addition to the parameters listed in Table I the following parameters were specified for this particular sample: $E_m^{(e)}=0.15$ eV, $E_m^{(h)}=0.15$ eV, $E_0^{(e)}=21$ meV, and $E_0^{(h)}=10.5$ meV.

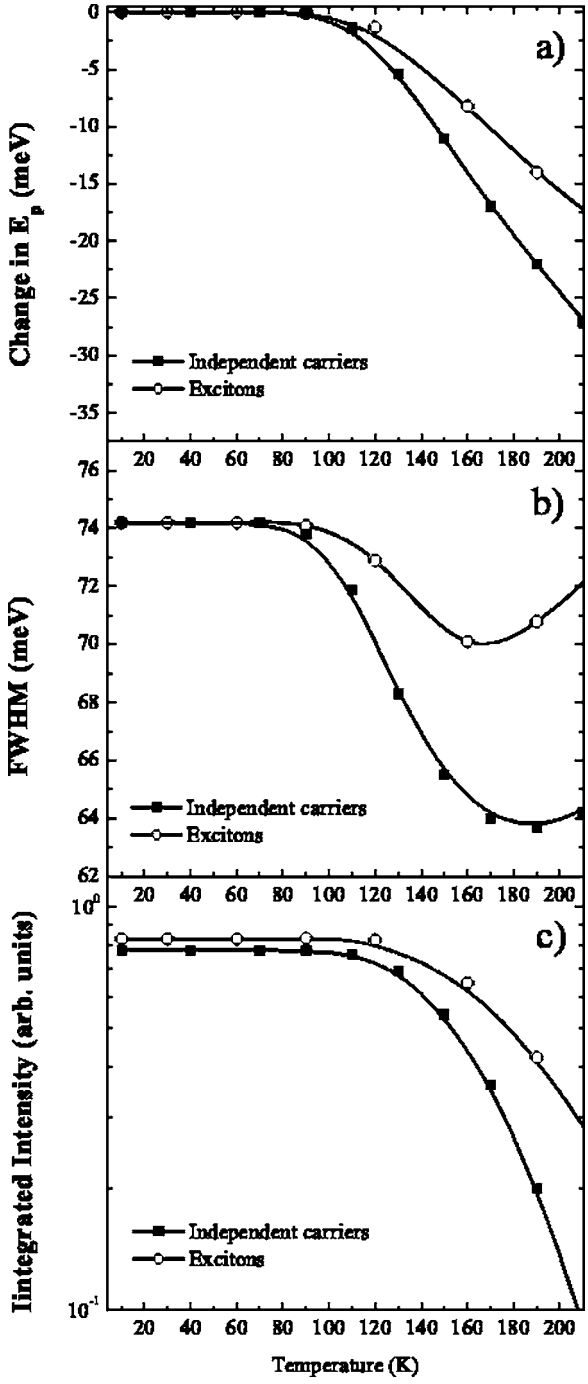

FIG. 5. Relative photoluminescence peak energy (a), the FWHM of the spectra (b), and integrated photoluminescence intensity (c) as a function of temperature calculated for sample No. 617 at the high excitation rate of $P=10^{19}$ cm^{-2} s^{-1}. Open circles and filled boxes correspond to the excitonic and nonexcitonic models, respectively. All sample parameters are the same as in Fig. 4.

$-E_0^2/kT$. These predictions are in reasonable agreement with the experimental data shown in Fig. 2.

The results shown in Fig. 4 were obtained for the excitation rate $P=10^{16}$ cm^{-2} s^{-1}, so in equilibrium a large fraction of the quantum dot ground states are unoccupied. In order to investigate the effect of the excitation rate on the optical properties, we repeated our calculations as a function of temperature for sample No. 617 for an excitation rate P greater by three orders of magnitude, noting that all the other input parameters remained unchanged. The results for the integrated photoluminescence intensity, photoluminescence peak

position, and the spectral linewidth for the high excitation rate are shown in Fig. 5.

The shift of the photoluminescence peak at 200 K for higher excitation rate [Fig. 4(a)] is predicted to be smaller by a factor of 2 compared to that at the lower excitation rate [Fig. 5(a)]. This is because at the lower excitation rate a significant fraction of the quantum dots are unoccupied so that carriers can relax to deeper energy states. Also the reduction of the photoluminescence linewidth [Fig. 5(b)] is less pronounced than that observed at the lower excitation rate [Fig. 4(b)]. These predictions are to an extent supported by the experimental data although the contrast between the high and low excitation data is not as pronounced as the theoretical predictions. We also predict a significant difference in the temperature dependence of the integrated intensity for the high and for the low excitation density [compare Figs. 5(c) and 4(c)] at temperatures approaching 200 K. For the low excitation density we predict an overall decrease in the integrated intensity of nearly three orders of magnitude as the temperature is increased; whereas we predict this decrease to be reduced to about an order of magnitude for the higher excitation density. Again these predictions are to an extent born out by the experimental data but not to quite the extent predicted. It should also be stressed that such an effect could also be produced experimentally by a degree of saturation of the centers in the barriers responsible for nonradiative recombination.

However, as described earlier, the optical properties are not always as sensitive to increased temperature as we have described for sample No. 617. In particular, some of our samples, such as No. 592, exhibit almost no redshift and no narrowing of the photoluminescence spectrum with increased temperature. Using our model for independent electrons and holes we obtain reasonable agreement between the predictions of the model, Figs. 6 and 7, and the experimental results for No. 592 (Fig. 2).

The changes in the temperature-dependent photoluminescence spectra are much smaller in comparison with sample No. 617. In particular, the predicted shift of the peak of the photoluminescence spectrum with increasing temperature is $\sim$10 meV at $T=200$ K [Fig. 6(a)] and there is virtually no change in the FWHM of the spectra [Fig. 6(b)]. The reason for this difference in behavior of the two samples is due to the different electronic structure of the quantum dots caused, as discussed earlier, by the difference in quantum dot sizes. The increase of the confinement energies, E_m, causes an increase of the activation energies required for the thermal release of carriers from the quantum dots. In addition, the energy distribution of the quantum dot ground states narrows with increasing dot size.[18] As a consequence the relatively small changes in the peak energy and FWHM of the spectra of No. 592 are observed. We would like to draw a parallel between this result and the recent work of Sanguinetti *et al.*,[23] where an observation of kinetic effects in the T-dependent PL spectra was attributed to the presence of the wetting layer (WL). In Ref. 23 the temperature-induced properties similar to those of sample No. 617 were observed for the sample containing the WL and were not seen for a sample without the WL. However, our experimental results for sample No. 592 suggest that the presence of the WL itself does not ensure an observation of the kinetic effects in T-dependent PL spectra. Therefore, the role of WL in the overall carrier dynamics should be further clarified.

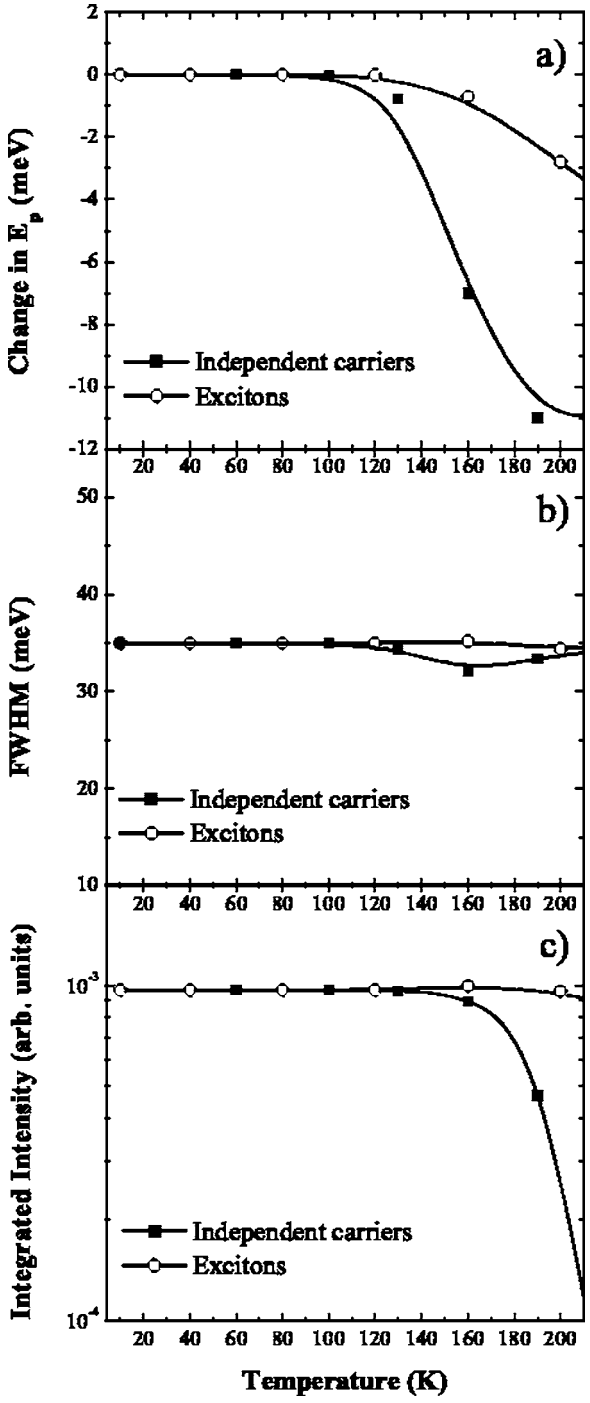

FIG. 6. Relative photoluminescence peak energy (a), the FWHM of the spectra (b), and integrated photoluminescence intensity (c) as a function of temperature calculated for sample No. 592 at the low excitation rate of $P=10^{16}$ cm^{-2} s^{-1}. Open circles and filled boxes correspond to the excitonic and nonexcitonic models, respectively. In addition to the parameters listed in Table I the following parameters were specified for this particular sample: $E_m^{(e)}=0.23$ eV, $E_m^{(h)}=0.19$ eV, $E_0^{(e)}=9.35$ meV, and $E_0^{(h)}=5.5$ meV.

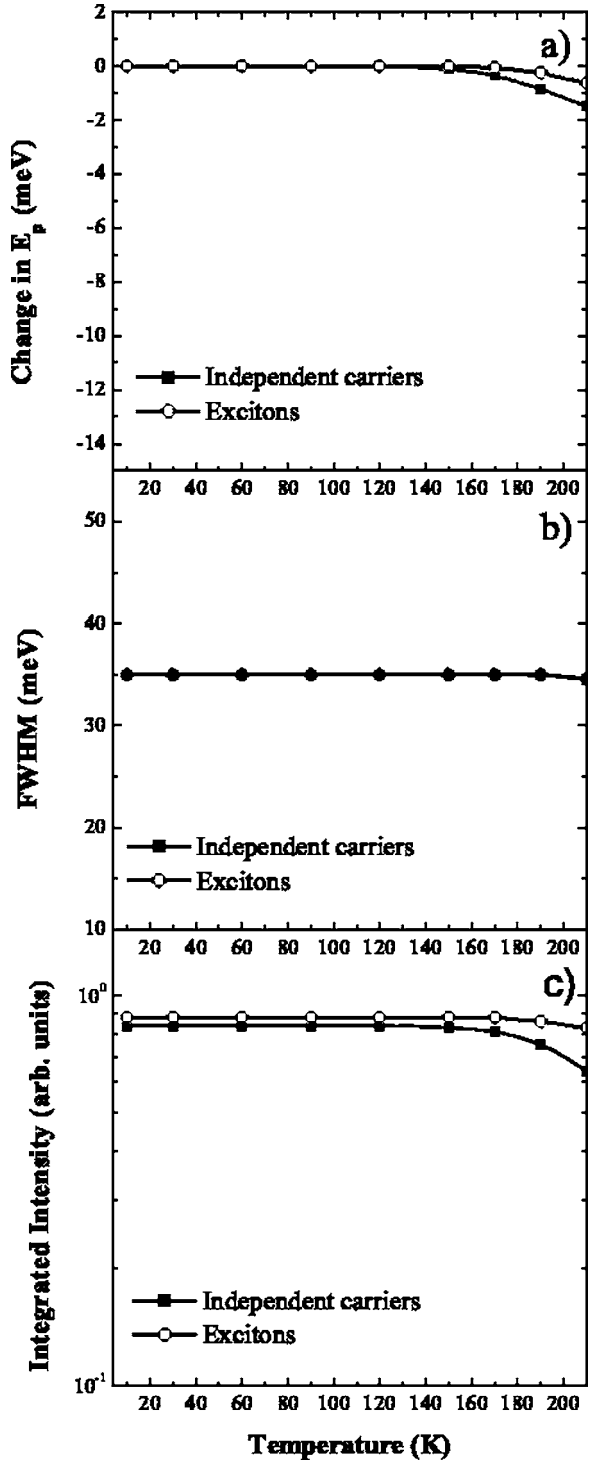

FIG. 7. Relative photoluminescence peak energy (a), the FWHM of the spectra (b), and integrated photoluminescence intensity (c) as a function of temperature calculated for sample No. 592 at the high excitation rate of $P=10^{19}$ cm^{-2} s^{-1}. Open circles and filled boxes correspond to the excitonic and nonexcitonic models, respectively. All sample parameters are the same as in Fig. 6.

So far the results that we have presented have been modeled with the set of rate equations given in Sec. IV A, in which the electrons and holes are treated independently. The low excitation density optical properties and their interpretation are not new and they can be found in many of the previous publications, in particular, in Refs. 10, 11, 13, 16, and 17. But as discussed earlier these theoretical treatments were based on a model where the electron-hole correlation is maintained during the carrier escape and recapture processes. Therefore, it is desirable to find out how crucial this assumption of the excitonic character of the electron-hole pairs is for the predicted optical properties. In order to address this problem we repeated our calculations using the exciton model described in Sec. IV B and, in particular, we pay attention to the predictions of the two models as a function of excitation density. As the optical properties of sample No. 617 are much more sensitive to the thermally activated carrier escape processes we concentrate on the excitation density dependence of the predicted behavior of this sample using the two models.

The predicted results for the photoluminescence intensity obtained with the two models are shown in Figs. 5(c) and 4(c) for sample No. 617 for high and low excitation densities, respectively. As already stated at the lowest temperatures the photogenerated carriers decay by radiative recombination in the quantum dots, thus the predictions of the two models are identical for low temperatures. The difference in the predictions of the two models becomes pronounced at higher temperatures when a significant fraction of the quantum dots are no longer occupied because of thermal excitation into the barrier and subsequent nonradiative or radiative loss in the barriers. In the exciton description the recombination partner for an electron or hole is always available, whereas in the case of separate electrons and holes the probability of an electron or hole finding a recombination partner in the same dot decreases with temperature, thus increasing the chance for nonradiative recombination. As a result, depending on the excitation density, it is anticipated that at high temperatures the photoluminescence intensity predicted by the exciton model will be much larger than that calculated for the independent electron and hole model. Specifically the independent electron-hole model predicts a reduction of almost three orders of magnitude in the photoluminescence intensity for the temperature range between 0 and 200 K at the low excitation rate [Fig. 4(c)]. Whereas at the high excitation rate, the photoluminescence intensity is predicted to decrease by less than one order of magnitude over the same temperature range [Fig. 5(c)]. In contrast the exciton model does not predict any difference in the thermal quenching of the photoluminescence intensity for the different excitation densities. The experimental data [Fig. 2] agree qualitatively with these differences in reductions of the two models but, again, not to the precise extent predicted. Therefore we conclude that although the exciton model is able to describe many of the optical properties, it fails to account for the excitation density dependence of the thermal quenching of the photoluminescence intensity. Whereas the model based on the uncorrelated electrons and holes is, to an extent, able to describe all the observed optical properties. In summary, the experimental data shown in Fig. 2(c) show that the thermal quenching depends on excitation power and is more pronounced for the low excitation power compared with the higher excitation power in contrast to the predictions of the exciton model. We therefore conclude that at elevated tem-

peratures the independent particle model provides the more realistic description, even though the agreement between our experimental data and the calculated behavior is not perfect. However, it must be pointed out that no attempts have been made to obtain better agreement by adjusting any of the parameters used in the equations.

VI. CONCLUSIONS

We have carried out experimental and theoretical studies of the temperature-dependent optical properties of InAs/GaAs quantum dots paying particular attention to the nature of the carrier escape and relaxation processes. The measured optical properties show distinct variations with excitation density that are best described by the theoretical model if the carriers are treated as independent electrons and holes rather than correlated electron-hole pairs (excitons).

ACKNOWLEDGMENTS

The authors would like to thank the Deutsche Forschungsgemeinschaft, European Community [IP "FULLSPECTRUM" (Ref. N: SES6-CT-2003-502620)], and to the Founds der Chemischen Industrie for financial support of various parts of this work. P.D. would like to thank the Physikalisch-Technische Bundesanstalt for their support.

*Email address: philip.dawson@manchester.ac.uk

[1] D. Bimberg, M. Grundmann, and N. N. Ledentsov, *Quantum Dot Heterostructures* (Wiley, New York, 1999).
[2] M. S. Skolnick and D. J. Mowbray, Physica E (Amsterdam) **21**, 155 (2004).
[3] S. Chichibu, K. Wada, and S. Nakamura, Appl. Phys. Lett. **71**, 2346 (1997).
[4] D. I. Lubyshev, P. P. Gonzalez-Borrero, E. Marega, E. Petitprez, N. L. Scala, and P. Basmaji, Appl. Phys. Lett. **68**, 205 (1996).
[5] S. Fafard, S. Raymond, G. Wang, R. Leon, D. Leonard, S. Charbonneau, J. L. Merz, P. M. Petroff, and J. E. Bowers, Surf. Sci. **361/362**, 778 (1996).
[6] Z. Y. Xu, Z. D. Lu, X. P. Yang, Z. L. Yuan, B. Z. Zheng, J. Z. Xu, W. K. Ge, Y. Wang, J. Wang, and L. L. Chang, Phys. Rev. B **54**, 11528 (1996).
[7] L. Brusaferri, S. Sanguinetti, E. Grilli, M. Guzzi, A. Bignazzi, F. Bogani, L. Carraresi, M. Colocci, A. Bosacchi, and P. Frigeri, Appl. Phys. Lett. **69**, 3354 (1996).
[8] Y. T. Dai, J. C. Fan, Y. F. Chen, R. M. Lin, S. C. Lee, and H. H. Lin, J. Appl. Phys. **82**, 4489 (1997).
[9] Z. Y. Xu, Z. D. Lu, Z. L. Yuan, X. P. Yang, B. Z. Zheng, J. Z. Xu, W. K. Ge, Y. Wang, J. Wang, and L. L. Chang, Superlattices Microstruct. **23**, 381 (1998).
[10] H. Lee, W. Yang, and P. Sercel, Phys. Rev. B **55**, 9757 (1997).
[11] S. Sanguinetti, M. Henini, M. Gyassi Alessi, M. Capizzi, P. Frigeri, and S. Franchi, Phys. Rev. B **60**, 8276 (1999).
[12] A. Polimeni, A. Patane, M. Henini, L. Eaves, and P. C. Main, Phys. Rev. B **59**, 5064 (1999).
[13] W. Yang, R. R. Lowe-Webb, H. Lee, and P. C. Sercel, Phys. Rev. B **56**, 13314 (1997).
[14] H. Y. Liu, B. Xu, Q. Gong, D. Ding, F. Q. Liu, Y. H. Chen, W. H. Jiang, X. L. Ye, Y. F. Li, and Z. Z. Sun, J. Cryst. Growth **210**, 451 (2000).
[15] R. Heitz, I. Mukhameetzhanov, A. Madukar, A. Hoffmann, and D. Bomberg, J. Electron. Mater. **28**, 520 (1999).
[16] D. P. Popescu, P. G. Eliseev, A. Stintz, and K. J. Malloy, Semicond. Sci. Technol. **19**, 33 (2004).
[17] F. V. de Sates, J. M. R. Cruz, S. W. de Silva, M. A. G. Soler, P. C. Morais, M. J. da Silva, A. A. Quivy, and J. R. Leite, J. Appl. Phys. **94**, 1787 (2003).
[18] J. A. Barker and E. P. O'Reilly, Phys. Rev. B **61**, 13840 (2000).
[19] I. Vurgaftman, J. R. Meyer, and L. R. Ram-Mohan, J. Appl. Phys. **89**, 5815 (2001).
[20] J. Shumway, A. J. Williamson, A. Zunger, A. Passaseo, M. DeGiorgi, R. Cingolani, M. Catalano, and P. Crozier, Phys. Rev. B **64**, 125302 (2001).
[21] B. Ohnesorge, M. Albrecht, J. Oshinowo, A. Forchel, and Y. Arakawa, Phys. Rev. B **54**, 11532 (1996).
[22] R. Heitz, M. Veit, N. N. Ledentsov, A. Hoffmann, D. Bimberg, V. M. Ustinov, P. S. Kop'ev, and Z. I. Alferov, Phys. Rev. B **56**, 10435 (1997).
[23] S. Sanguinetti, T. Mano, M. Oshima, T. Tateno, M. Wakaki, and N. Koguchi, Appl. Phys. Lett. **81**, 3067 (2002).